Micro Size Tapered Silica Fibers for Sensing Applications

Roddy E. Ramos Gonzáles, Enver F. Chillcce, Luiz C. Barbosa

Instituto de Física Gleb "Wataghin", Unicamp, Campinas, SP, 13083-970, Brazil.

ABSTRACT

In this work we show results of controlled tapered fibers using a Vytran instrument. The tapered silica fibers were produced by pulling a 50μm length by heating time. The minimum taper diameter was around 3μm and the maximum taper length was around 600μm. The evanescent field effect, in the near infra red (NIR) region, was observed to the tapers with diameter inferior to 15μm. These micro-size tapers no modify the waveguide dispersion spectra. This device could be used to splice a conventional fiber to photonic crystal fibers and also as liquid and gas sensors In this work is reported a fiber optic sensor in the form of taper using the concept of the evanescent field. We show the sensor sensitivity using different liquid materials.

INTRODUCTION

Taper fiber is a *cone-like* (or conical-like) optical fiber shape with variable diameter. It consists of transition regions, where the fiber diameter decreases gradually until the value of the "waist", which is its main quality, as is shown in the Figure 1.

We can use several definitions to terms to emphasize their different properties, such as: Sub wavelength Waveguide [1]; Sub wavelength Optical Wire [2]; Sub wavelength-Diameter Silica Wire [3]; Sub wavelength Diameter Fiber Taper [4]; Photonic Wire Waveguide [5]; Photonic Wire [6]; Photonic Nanowire [7]; Optical Nanowires [8]; Optical Fiber Nanowires [9]; Tapered (Optical) Fiber [10]; Fiber Taper [11]; Submicron-Diameter Silica Fiber [12]; Ultra-Thin Optical Fibers [13]; Optical Nano fiber [14]; Optical Microfibers [15]; Submicron Fiber Waveguides [16]. The main peculiarity of a fiber taper is that in the waist region a significant portion of the light propagates outside of the fiber. In a simple way, it can be explained by the following idea, the light is guided by total internal reflection that occurs at the interface between the waveguide and the surrounding media. The light intensity does not drop to zero immediately at the interface but, decreases exponentially (and disappears) out of the optical guide (the field of light outside the optical guide is called the evanescent field). The depth of light penetration during total internal reflection depends on the configuration of the fiber taper is usually greater or is of the order of the wavelength of light. The propagation of light in a submicron diameter fiber is governed by the equations of propagation which is different than a conventional optical fiber [17, 18].

Here, the analysis is done in the region where the wavelength λ varies between 0.4 and 1.7 μm. We calculate the wavelength λ_m for which the fiber taper have submicron size, once the smaller fiber diameter Φ_{Fm} is equal to the waist d_{NN}, we consider the fiber taper core diameter Φ_{Nm} equals to λ_m : $\lambda_m = \Phi_{Fm} = (8.2/125) \cdot \Phi_{Fm} = (125/4.1) \cdot d_{NN}$.

Thus we work with fibers which taper at the waist core d_{NN} is smaller than the wavelength, $\Phi_{Nm} < \lambda$, in the analysis region.
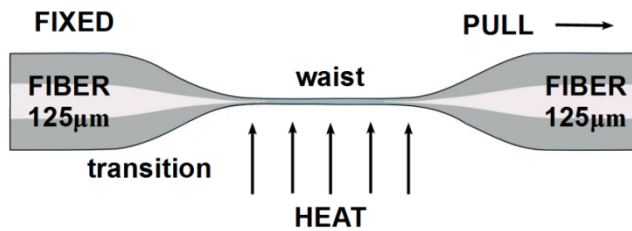
Fig. 1.- *Scheme of a fiber taper.*

FABRICATION

The fabrication of fiber taper has been done in a VYTRAN - Filament Fusion Splicing System equipment, Model FFS-2000. The optical fiber generally consists of a core, a shell and a protective coating. The coating is removed usually using acrylate. Then, the bare fiber is fixed at both ends (one fixed and one mobile), Figure 1. The middle of the fiber is heated by heat produced by an electrical resistance (filament), while the extreme mobile moves in the opposite direction. The glass heats up and the fiber is pulled until its diameter decreases. Being extremely thin, the fiber taper is fragile. So, after the pulling procedure, it is mounted on a structure and is never more is separated from this assembly. Dust particles can be adsorbed on the surface of the fiber taper near the waistline. If the laser energy coupled into the fiber in significant way, the dust particles can scatter the light and creates an evanescent field that can heat and destruct the waist of the fiber taper.
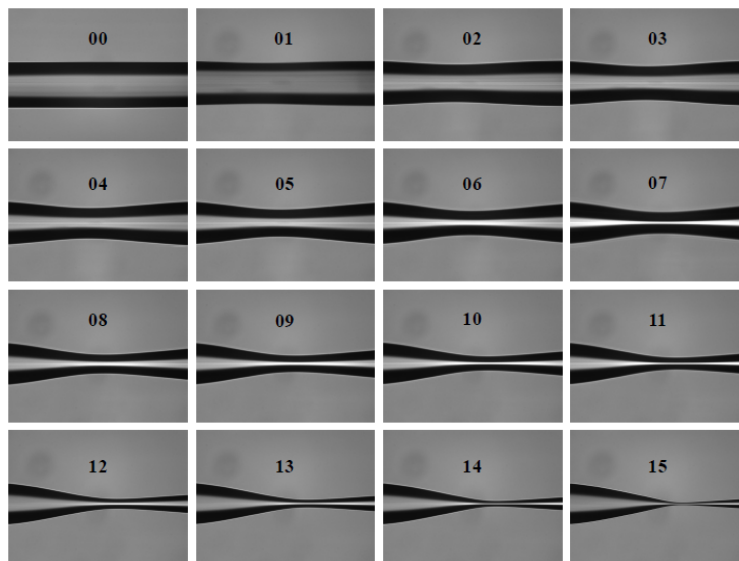
Fig. 2.- *Photos from the assembly of fiber taper, SMF, which is shown in the sequence.*

To avoid that, the fiber taper is pulled in environments free of dust (clean enough). We manufacture fiber tapers with waists size smaller than 15 μm. For smallest fiber size we got a lot
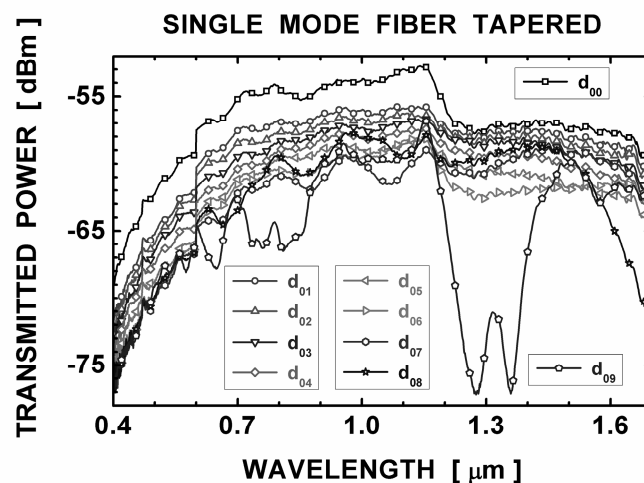
of troubles due to their fragility mainly its can broke at the assembly time or characterization. Figure 2 shows in sequence the process as a commercial single-mode optical fiber is transformed into a fiber-taper (Initial: step 00 – d_{NN} = 125 µm - Final: step 15 – d_{NN} = 9.3 µm). The photographs were taken by the equipment which also allows us to measure the dimensions of the fiber taper, especially at the waist. We observed the "deformation" of the fiber in the process, the left end of the fiber remains fixed while the right end is pulled to the desired final dimension. At fifteen steps we obtained with d_{NN} = 9.3 µm.
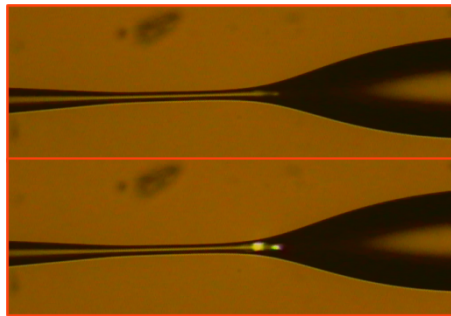
Fig. 3.- *Photos of the fiber taper. (Top) No signal. Signal of a source of white light (Bottom).*

Figure 3 shows a fiber taper when light is inserted through it. We observed that a portion of light is emitted out of the fiber. Depending on the geometry this effect is not noticeable. During manufacturing, we make the signal measurement through the fiber by measuring its transmitted power, using a white light source and an optical spectrum analyzer OSA.

Figure 4 shows the transmitted power behavior through the fiber taper single-mode for different waist sizes d_{NN} as a function of wavelength λ. The values of d_{NN} are in decreasing order, $d_{00} > d_{01} > \ldots > d_{08} > d_{09}$, and d_{00} = 125 µm. i.e., a single-mode fiber. The d_{NN} values were: d_{01} = 60.1 µm, d_{02} = 53.3 µm, d_{03} = 47.1 µm, d_{04} = 40.9 µm, d_{05} = 34.7 µm, d_{06} = 27.9 µm, d_{07} = 22.3 µm, d_{08} = 16.7 µm and d_{09} = 9.3 µm.

Fig. 4.- *Transmitted power of the fiber taper waist with d_{NN}.*

We note that for $d_{00} \geq d_{NN} \geq d_{05}$ the transmitted power behavior is the same. That is, when the fiber diameter is reduced to a quarter of its size the transmission of light through it as a function of λ has the same behavior, but with lower intensity. For the d_{06} to d_{08} the fiber behavior starts to vary with λ, in a no standard way. For d_{09} the power behavior are oscillations. The power has fallen in intensity, which are clearly the two absorption peaks of water, approximately 1.24 and 1.38 μm. All these power measurements were made with air around the fiber taper.

RESULTS

Figure 5 shows the fiber taper being applied as a sensor. Taking as advantage its waist size, a liquid material is placed in the region of its waist (a few drops can sufficiently cover the region).

Fig. 5.- *Fiber taper assembly waist d_{NN} applied as a sensor.*

We measure what happens to the signal that is guided through the fiber taper. The difference of media (silica-liquid) causes the signal changes to certain wavelengths. Figure 6 shows the behavior of the transmitted power when we use other media (such as water, alcohol methylol and PbS quantum dots dissolved in toluene - PbS QDs) around a single mode fiber taper $d_{NN} = 9.3$ as a function of wavelength. We observed that the power behavior of when we put water is similar to alcohol methylol, with the difference that the fall in water $\lambda = 1.38$ μm is more pronounced.
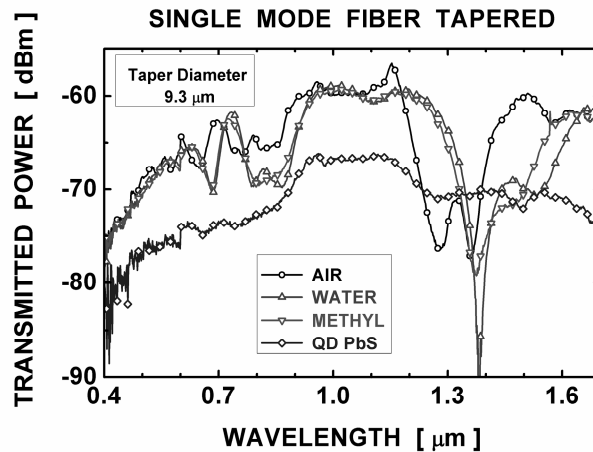
Fig. 6. - *Transmitted power of the fiber taper for different materials.*

When it is placed PbS QDs in the waist region, the behavior is different. In the region from 1.3 μm to 1.6 μm the power is almost constant, we observed a fall of approximately λ = 1.5 μm which is due to the absorption peak of PbS QDs located at 1.474 μm. We used the same single-mode fiber taper for these measurements. After each measurement the fiber taper was cleaned with isopropyl alcohol. The transmission power of the air measured at the beginning of the experiment was used as standard for comparison each time the fiber taper was clean, where we get the same spectrum. Once placing the PbS QDs in the fiber taper, we could not remove it (QDs) without damaging the fragile waist of the fiber taper.

Figure 7 show the behavior of the normalized transmittance, compared to air, when other media were used (water, isopropyl alcohol and ethanol alcohol) around the single-mode fiber taper whose waist is 14 μm. We observed this behavior as a function of wavelength. We make a comparison of the water measurements and isopropanol as the two mixtures of them. In the figure 7a we observed in the region where the fiber is single mode (λ ≥ 1.3 μm). For example, comparing the intensities in λ = 1.3 μm isopropyl response increases as we grow the
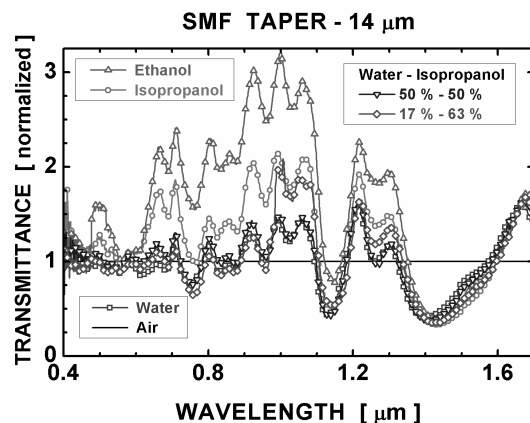

Fig. 7.- *Transmittance of the fiber taper for different materials*

amount of water in the solution, then the transmittance decreases. For λ = 1.5 μm, unlike the water in the solution increases the transmittance increases. Figure 8 shows the transmittance

behavior when we use mixtures of ethanol with water around the fiber taper whose waist is 14 μm. We observed this behavior as a function of wavelength. We make a comparison of curves for seven different concentrations. In them we could see, especially in the infrared region from 2.0 μm to 2.2 μm. This measurement was made with a high resolution spectrometer for this specific region. We observed that when we increase the water concentration, the transmittance is higher, i.e., when we increase the ethanol concentration in the mixture, the transmittance absorption peaks intensity characteristic of C-OH decreases.
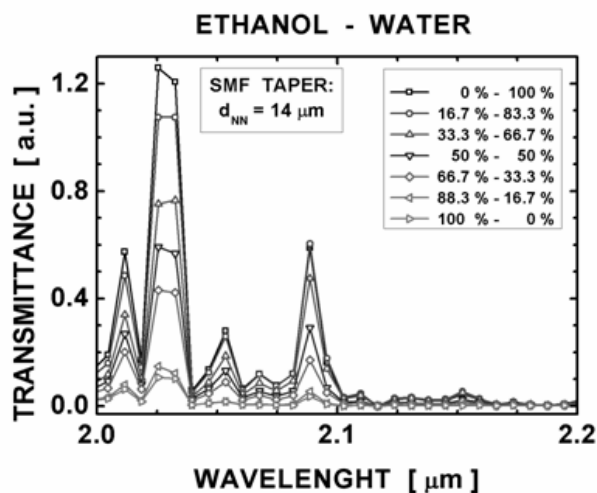

Fig. 8.- *Transmittance of the fiber taper for different mixtures of ethanol with water.*

CONCLUSION

With the changes in the spectra of the transmitted power and the transmittance, we reached the conclusion that the fabricated fiber taper by this method can be used as a sensor for liquids.

REFERENCES

[1]   Mark A. Foster and Alexander L. Gaeta, "*Ultra-low threshold supercontinuum generation in sub-wavelength waveguides*"; Opt. Express Vol. 12, No. 14, pp. 3137- 3143, (2004).
[2]   Yongmin Jung, Gilberto Brambilla and David J. Richardson; "*Broadband single-mode operation of standard optical fibers by using a sub-wavelength optical wire filter*", Opt. Express Vol. 16, No. 19, pp. 14661–14667, (2008).
[3]   Limin Tong, Rafael R. Gattass, Jonathan B. Ashcom, Sailing He, Jingyi Lou, Mengyan Shen, Iva Maxwell and Eric Mazur; "*Subwavelength-diamter silica wires for low-loss optical wave guiding*", Nature, Vol. 426, pp. 816 – 819, (2003).
[4]   Lei Zhang, Fuxing Gu, Jingyi Lou, Xuefeng Yin and Limin Tong, "*Fast detection of humidity with a subwavelength-diameter fiber taper coated with gelatin film*", Opt. Express Vol. 16, No. 17, pp. 13349-13353, (2008).
[5]   Richard L. Espinola, Jerry I. Dadap, Richard M. Osgood Jr., Sharee J. McNab and Yurii A. Vlasov; "*C-band wavelength conversion in silicon photonic wire waveguides*", Opt. Express Vol. 13, No. 11, pp. 4341 – 4349, (2005).
[6]   Yannick K. Lizé, Eric C. Mägi, Vahid G. Ta'eed, Jeremy A. Bolger, Paul Steinvurzel, and Benjamin J. Eggleton; "*Microstructured optical fiber photonic wires with subwavelength core diameter*", Opt. Express, Vol. 12, No. 14, pp. 3209 – 3217, (2004).
[7]   Mark A. Foster, Amy C. Turner, Michal Lipson and Alexander L. Gaeta; "*Nonlinear optics in photonic nanowires*", Opt. Express, Vol. 16, No. 2, pp. 1300 – 1320, (2008).
[8]   G. A. Siviloglou, S. Suntsov, R. El-Ganainy, R. Iwanow, G. I. Stegeman and D. N. Christodoulides; "*Enchanced third-order nonlinear effects in optical AlGaAs nanowires*", Opt. Express, Vol. 14, No. 20, pp. 9377 – 9384, (2006).

[9] Optical Fibre Nanowires and Related Devices Group, Optoelectronics Research Centre, University of Southampton; www.orc.soton.ac.uk/ofnrd.html.

[10] C. M. B. Cordeiro, W. J. Wadsworth, T. A. Birks and P. St. J. Russell, "*Engineering the dispersion of tapered fibers for supercontinuum generation with a 1064 nm pump laser*", Opt. Lett., Vol. 30, No. 15, pp. 1980 – 1982, (2005).

[11] William J. Wadsworth, Arturo Ortigosa-Blanch, Jonathan C. Knight, Tim A. Birks, T.-P. Martin Man and Phillip St. J. Russell; "*Supercontinuum generation in photonic crystal fibers and optical fiber tapers: a novel light source*", J. Opt. Soc. Am. B, Vol. 19, No. 9, pp. 2148 – 2155, (2002).

[12] Lei Shi, Xianfeng Chen, Hongjuan Liu, Yuping Chen, Zhiqing Ye, Weijun Liao and Yuxing Xia; "*Fabrication of submicron-diameter silica fibers using electric strip heater*", Opt. Express Vol. 14, No. 12, pp. 5055 – 5060, (2006).

[13] G. Sagué, A. Baade and A. Rauschenbeutel, "*Blue-detuned evanescent field surface traps for neutral atoms based on mode interference in ultra-thin optical fibres*", New J. Phys., Vol. 10, 113008, 18 pp., (2008).

[14] K. P. Nayak, P. N. Melentiev, M. Morinaga, Fam Le Kien, V. I. Balykin and K. Hakuta; "*Optical nanofiber as an efficient tool for manipulating and probing atomic fluorescence*", Opt. Express, Vol. 15, No. 9, pp. 5431 – 5438, (2007).

[15] Fei Xu, Peter Horak and Gilberto Brambilla, "*Optical microfiber coil resonator refractometric sensor*", Opt. Express Vol. 15, No. 12, pp. 7888-7893, (2007).

[16] S. G. Leon-Saval, T. A. Birks, W. J. Wadsworth and P. St.J. Russell; "*Supercontinuum generation in submicron fibre waveguides*", Opt. Express Vol. 12, No. 13, pp. 2864 – 2869, (2004).

[17] Truong X. Tran and Fabio Biancalana, "*An accurate envelope equation for light propagation in photonic nanowires: new nonlinear effects*", Opt. Express, Vol. 17, No. 20, pp. 17934 – 17949, (2009).

[18] F. Biancalana, Tr. X. Tran, S. Stark, M. A. Schmidt, and P. S. Russell, "*Emergence of geometrical optical nonlinearities in photonic crystal fiber nanowires*", Physical Review Letters 105, 093904, (2010).